REGULAR ARTICLE

blood advances

Prognostic significance of *FCGR2B* expression for the response of DLBCL patients to rituximab or obinutuzumab treatment

Malgorzata Nowicka,[1,*] Laura K. Hilton,[2,3,*] Margaret Ashton-Key,[4,5] Chantal E. Hargreaves,[4] Chern Lee,[5] Russell Foxall,[6] Matthew J. Carter,[6] Stephen A. Beers,[6] Kathleen N. Potter,[4] Christopher R. Bolen,[7] Christian Klein,[8] Andrea Knapp,[1] Farheen Mir,[9] Matthew Rose-Zerilli,[4] Cathy Burton,[10] Wolfram Klapper,[11] David W. Scott,[2,12] Laurie H. Sehn,[2,12] Umberto Vitolo,[13] Maurizio Martelli,[14] Marek Trneny,[15] Christopher K. Rushton,[16] Graham W. Slack,[2] Pedro Farinha,[2] Jonathan C. Strefford,[4,†] Mikkel Z. Oestergaard,[1,†] Ryan D. Morin,[3,16,†] and Mark S. Cragg,[4,6,†]

[1]F. Hoffmann-La Roche Ltd, Basel, Switzerland; [2]BC Cancer Centre for Lymphoid Cancer, Vancouver, BC, Canada; [3]Canada's Michael Smith Genome Sciences Centre, Vancouver, BC, Canada; [4]School of Cancer Sciences, University of Southampton, Southampton, United Kingdom; [5]Southampton University Hospitals NHS Foundation Trust, Southampton, United Kingdom; [6]Antibody and Vaccine Group, Centre for Cancer Immunology, School of Cancer Sciences, University of Southampton, Faculty of Medicine, Southampton, United Kingdom; [7]Genentech, Inc., South San Francisco, CA; [8]Roche Innovation Center Zurich, Schlieren, Switzerland; [9]Royal Marsden Hospital, Sutton, United Kingdom; [10]St James's Institute of Oncology, Leeds, United Kingdom; [11]Department of Hematopathology, University of Schleswig-Holstein, Campus Kiel, Kiel, Germany; [12]Department of Medicine, University of British Columbia, Vancouver, BC, Canada; [13]Multidisciplinary Oncology Outpatient Clinic, Candiolo Cancer Institute, FPO-IRCCS, Candiolo, Italy; [14]Department of Translational and Precision Medicine, Hematology, Sapienza University, Rome, Italy; [15]1st Medical Faculty, Charles University, Prague, Czech Republic; and [16]Department of Molecular Biology and Biochemistry, Simon Fraser University, Burnaby, BC, Canada

Key Points

- High *FCGR2B* expression is associated with shorter survival in patients with DLBCL receiving rituximab (R)-CHOP but not obinutuzumab-CHOP.
- The inferior outcomes seen with R-CHOP are independent of established prognostic biomarkers, and associated with tumor-expressed FcγRIIB.

Fc γ receptor IIB (FcγRIIB) is an inhibitory molecule capable of reducing antibody immunotherapy efficacy. We hypothesized its expression could confer resistance in patients with diffuse large B-cell lymphoma (DLBCL) treated with anti-CD20 monoclonal antibody (mAb) chemoimmunotherapy, with outcomes varying depending on mAb (rituximab [R]/obinutuzumab [G]) because of different mechanisms of action. We evaluated correlates between *FCGR2B* messenger RNA and/or FcγRIIB protein expression and outcomes in 3 de novo DLBCL discovery cohorts treated with R plus cyclophosphamide, doxorubicin, vincristine, and prednisone (R-CHOP) reported by Arthur, Schmitz, and Reddy, and R-CHOP/G-CHOP-treated patients in the GOYA trial (NCT01287741). In the discovery cohorts, higher *FCGR2B* expression was associated with significantly shorter progression-free survival (PFS; Arthur: hazard ratio [HR], 1.09; 95% confidence interval [CI], 1.01-1.19; $P = .0360$; Schmitz: HR, 1.13; 95% CI, 1.02-1.26; $P = .0243$). Similar results were observed in GOYA with R-CHOP (HR, 1.26; 95% CI, 1.00-1.58; $P = .0455$), but not G-CHOP (HR, 0.91; 95% CI, 0.69-1.20; $P = .50$). A nonsignificant trend that high *FCGR2B* expression favored G-CHOP over R-CHOP was observed (HR, 0.67; 95% CI, 0.44-1.02; $P = .0622$); however, low *FCGR2B* expression favored R-CHOP (HR, 1.58; 95% CI, 1.00-2.50; $P = .0503$). In Arthur and GOYA, *FCGR2B* expression was associated with tumor FcγRIIB expression; correlating with shorter PFS for R-CHOP (HR, 2.17; 95% CI, 1.04-4.50; $P = .0378$), but not G-CHOP (HR, 1.37; 95% CI, 0.66-2.87; $P = .3997$). This effect was independent of established prognostic biomarkers. High FcγRIIB/*FCGR2B* expression has prognostic value

Submitted 17 March 2021; accepted 8 April 2021; published online 29 July 2021. DOI 10.1182/bloodadvances.2021004770.

*M.N. and L.K.H. contributed equally as lead authors.

†J.C.S., M.Z.O., R.D.M., and M.S.C. share senior authorship.

Qualified researchers may request access to individual patient level data through the clinical study data request platform (https://vivli.org/). Further details on Roche's criteria for eligible studies are available at https://vivli.org/members/ourmembers/. For further details on Roche's Global Policy on the Sharing of Clinical Information and how to request access to related clinical study documents, see https://www.roche.com/research_and_development/who_we_are_how_we_work/clinical_trials/our_commitment_to_data_sharing.htm. The GOYA RNA sequencing (RNA-Seq) data are available at the Gene Expression Omnibus (accession number: GSE125966; https://www.ncbi.nlm.nih.gov/geo/query/acc.cgi?acc=GSE125966).

The full-text version of this article contains a data supplement.

in R-treated patients with DLBCL and may confer differential responsiveness to R-CHOP/G-CHOP.

Introduction

The anti-CD20 monoclonal antibody (mAb) rituximab (R) has been used for the treatment of relapsed/refractory non-Hodgkin lymphomafor >20 years, becoming ubiquitous in the treatment of B-cell disorders spanning malignant and autoimmune pathologies.[1-3] This success highlights the utility of mAbs for disease treatment and CD20 as a therapeutic target. Despite the clinical benefits of R plus chemotherapy, a sizable proportion of patients are refractory to/relapse following treatment, inviting the next generation of mAb therapeutics for non-Hodgkin lymphoma.[2,4] The study of anti-CD20 mAbs has also identified important determinants of cell-surface antigens that are optimal for target cell deletion and has enabled key mechanisms of action of direct-targeting antibodies to be defined.[4]

Anti-CD20 mAbs affect target cells in vivo by 4 separate mechanisms: direct cell death, complement-dependent cytotoxicity (CDC), antibody-dependent cellular cytotoxicity (ADCC), and antibody-dependent cellular phagocytosis (ADCP).[4] Although the importance of each is debated, current evidence suggests that effector mechanisms mediated by Fc γ receptors (FcγR) are critical. Preclinical studies in mouse models strongly favor myeloid cells as the key effectors, operating through ADCP[5-9]; macrophages become activated by mAb-opsonized target cells through their activatory FcγR, resulting in target cell engulfment and destruction. Previous studies have shown that macrophages are a key determinant of antitumor treatment response,[10] indicating that macrophages (in some patients) can be harnessed for antitumor effects.[11,12] This was previously confirmed in the GOYA trial, which reported a correlation between high programmed death-ligand 1 expression, a marker of macrophage activation, and improved response after anti-CD20 chemoimmunotherapy in a subset of patients.[13] FcγR IIB (FcγRIIB), the sole inhibitory FcγR, is thought to limit ADCP by reducing activatory FcγR signaling in a Src homology 2 domain-containing inositol phosphatase- and Src homology 2-containing tyrosine phosphatase-1-dependent manner.[14] In primary cultures of chronic lymphocytic leukemia (CLL) cells, FcγR-dependent macrophage ADCP was shown to correlate with clinical response, with resistance to ADCP resulting from reduced signaling activity through the activating FcγRs, and attributed to dominance of FcγRIIB.[15] It should be recognized that natural killer (NK) cells (presumably through ADCC) may also represent important effectors in humans because recent studies have indicated a prognostic impact of NK cell numbers in chemoimmunotherapy-treated patients with follicular lymphoma (FL) and diffuse large B-cell lymphoma (DLBCL).[16]

In part, these hypotheses regarding critical effector mechanisms have been informed by clinical experience with second generation anti-CD20 mAbs, such as ofatumumab and obinutuzumab (GA101 [G]). Ofatumumab is a fully human mAb with enhanced CDC activity, but has not demonstrated clinical improvement over R.[17-19] In contrast, the humanized mAb, G, has shown improved activity over R in CLL[20] and FL,[21,22] but not DLBCL.[23,24] The augmented activity of G has several possible explanations. First, G is a type II anti-CD20 mAb, which, unlike ofatumumab, does not cluster CD20, precipitate complement component 1q binding, or cause efficient CDC. Rather, such type II mAbs elicit nonapoptotic, lysosomal cell death, at least in some cell types.[25-28] Second, G possesses a glycoengineered afucosylated Fc region with higher affinity binding to FcγRIII, resulting in an increased capacity to elicit both NK-mediated ADCC and myeloid-mediated ADCP.[29,30] Finally, type II mAbs do not rapidly internalize from the cell surface, unlike their type I counterparts, such as R; this rapid internalization experienced by type I mAbs limits all of their Fc-mediated effector functions.[7,31] Recently, it was shown that reduced FcγRIIB-mediated internalization of G relative to R on CLL cells leads to increased phagocytosis by primary macrophages in an FcγRI-dependent manner.[32] It remains unclear which of these phenomena elicits the improvement in efficacy; however, in preclinical models in which lysosomal cell death is absent and afucosylation is lacking, type II mAbs significantly outperform R, presumably because of lack of internalization.[7,8] We previously showed that this internalization is augmented by the coexpression of FcγRIIB on the B-cell surface, resulting in degradation of the mAb in lysosomes.[31] This effect was greatly reduced with G (fucosylated and afucosylated) compared with R or ofatumumab, and was confirmed in primary clinical samples, including DLBCL.[31,33]

Through whole-genome sequencing of DLBCL, we recently described recurrent focal amplifications of *FCGR2B* in a subset of germinal center B-cell (GCB) DLBCLs, which drive elevated messenger RNA and protein expression. These mutations and high *FCGR2B* expression were associated with inferior outcomes in patients treated with R plus cyclophosphamide, doxorubicin, vincristine, and prednisone (CHOP).[34] Owing to the variable expression of *FCGR2B* in DLBCL, contributed in part by genetic alterations, we hypothesized that high FcγRIIB expression on malignant cells could confer resistance to anti-CD20 mAbs in DLBCL, with a differential impact on the efficacy of R and G. In this retrospectively designed analysis, we evaluated the gene and protein expression of FcγRIIB in a series of large clinical cohorts of DLBCL, and examined associations with response in R-CHOP- and G-CHOP-treated patients.

Methods

Data sets

We assessed the prognostic effect of FcγRIIB in DLBCL in 3 discovery cohorts of de novo DLBCL uniformly treated with R-CHOP[34-36] and in the GOYA trial, which compared R-CHOP with G-CHOP.[23,24]

We analyzed data from 404 patients from the Arthur cohort,[34] 554/574 patients from the Schmitz cohort (20 omitted patients were biopsied at relapse and treated with ibrutinib),[35] and 1001 patients from the Reddy cohort.[36]

A Study of Obinutuzumab in Combination With CHOP Chemotherapy Versus Rituximab With CHOP in Participants With CD20-Positive Diffuse Large B-Cell Lymphoma (GOYA) (NCT01287741) was a phase 3, multicenter, open-label, randomized trial. Full details of its design and primary end points were published previously.[23,24] In

brief, previously untreated patients with DLBCL were randomized to receive 8 21-day cycles of G or R plus 6 or 8 cycles of CHOP. The number of CHOP cycles for both arms was agreed in advance with each study site. If 6 CHOP cycles were administered, the mAb was administered as monotherapy during cycles 7 and 8. The primary end point was investigator-assessed progression-free survival (PFS). The trial protocol was approved by local or national ethics committees according to the laws of each country, and the trial was undertaken in accordance with the Declaration of Helsinki. Written informed consent was provided by all patients. We used data from the final analysis of GOYA (clinical cutoff date: 31 January 2018), which were available for 1414 patients.[24]

Available and analyzed biomarker and outcome data from these clinical cohorts are summarized in supplemental Table 1. Median duration of follow-up and patient demographic and baseline characteristics are presented in Table 1.

RNA sequencing

RNA from the Arthur and Schmitz cohorts was extracted from frozen tumors. In the Reddy cohort, RNA was extracted from formalin-fixed paraffin-embedded (FFPE) samples. Details of sample processing were described previously.[34-36] In GOYA, RNA was extracted from pretreatment FFPE tissue using the RNeasy FFPE kit (Qiagen,

Table 1. Demographic and baseline characteristics of DLBCL patients (all patients [ITT population] and BEP population) in the 3 discovery cohorts and the GOYA study

	Arthur		Schmitz		Reddy		GOYA	
Characteristic*	**All (N = 404)**	**BEP RNA-seq (n = 372)**	**All (N = 554)**	**BEP RNA-seq (n = 234)**	**All (N = 1001)**	**BEP RNA-seq (n = 455)**	**All (N = 1414)**	**BEP RNA-seq (n = 552)**
Median follow-up, y	11.7	11.5	10.5	10.5	10.4	8.9	4.0	4.1
Age, n	404	372	546	234	950	448	1414	552
Median (range), y	64 (16-92)	64 (16-92)	62 (14-92)	61 (16-92)	62 (3.1-93.4)	63 (3.1-93.4)	62 (18-86)	63 (18-85)
Female	153 (37.9)	143 (38.4)	241 (43.5)	95 (40.6)	434 (43.5)†	196 (43.1)	664 (47.0)	264 (47.8)
IPI, n	385	354	339	189	761	388	1414	552
Low	128 (33.3)	118 (33.3)	103 (30.4)	77 (40.7)	244 (32.1)	120 (30.9)	282 (19.9)	107 (19.4)
Low-intermediate	105 (27.3)	97 (27.4)	87 (25.7)	45 (23.8)	180 (23.7)	94 (24.2)	500 (35.4)	194 (35.1)
High-intermediate	71 (18.4)	64 (18.1)	84 (24.8)	44 (23.3)	192 (25.2)	101 (26.0)	412 (29.1)	161 (29.2)
High	81 (21.0)	75 (21.2)	65 (19.2)	23 (12.2)	145 (19.1)	73 (18.8)	220 (15.6)	90 (16.3)
Ann Arbor stage at diagnosis, n	404	372	458	231	974	448	1413	552
I/II	180 (44.6)	165 (44.3)	200 (43.7)	109 (47.2)	384 (39.4)	176 (39.3)	340 (24.1)	134 (24.3)
III/IV	224 (55.4)	207 (55.7)	258 (56.3)	122 (52.8)	590 (60.6)	272 (60.7)	1073 (75.9)	418 (75.7)
COO, n	388	364	554	234	775	455	933	538
GCB	217 (55.9)	204 (56.0)	164 (29.6)	110 (47.0)	331 (42.7)	197 (43.3)	540 (57.9)	298 (55.4)
ABC	129 (33.3)	120 (33.0)	279 (50.4)	82 (35.0)	313 (40.4)	187 (41.1)	243 (26.1)	151 (28.1)
Unclassified	42 (10.8)	40 (11.0)	111 (20.0)	42 (18.0)	131 (16.9)	71 (15.6)	150 (16.1)	89 (16.5)
DHITsig, n	204	204	134	107	207	197	298	298
Positive	60 (29.4)	60 (29.4)	24 (17.9)	21 (19.6)	57 (27.5)	53 (26.9)	32 (10.7)	32 (10.7)
Negative	144 (70.6)	144 (70.6)	110 (82.1)	86 (80.4)	150 (72.5)	144 (73.1)	266 (89.3)	266 (89.26)
BCL2 by IHC, n	364	343	0	0	462	230	755	433
Positive	245 (67.3)	235 (68.5)	–	–	323 (69.9)	172 (74.8)	363 (48.1)	206 (47.6)
Negative	119 (32.7)	108 (31.5)	–	–	139 (30.1)	58 (25.2)	392 (51.9)	227 (52.4)
Number of chemotherapy cycles, n	–	–	–	–	–	–	1414	552
6	–	–	–	–	–	–	1045 (73.9)	402 (72.8)
8	–	–	–	–	–	–	369 (26.1)	150 (27.2)
Geographic region, n							1414	552
Asia	–	–	–	–	–	–	514 (36.4)	89 (16.1)
Eastern Europe	–	–	–	–	–	–	196 (13.9)	122 (22.1)
Western Europe	–	–	–	–	–	–	426 (30.1)	216 (39.1)
North America	–	–	–	–	–	–	216 (15.3)	93 (16.9)
Other	–	–	–	–	–	–	62 (4.4)	32 (5.8)

* All data are n (%) unless otherwise stated.
† Data missing for n = 3.
DHITsig, double-hit gene expression signature; ITT, intent-to-treat.

Hilden, Germany). Whole transcriptome gene expression was assayed using Illumina TruSeq RNA Access.

For the Reddy, Arthur, and GOYA cohorts, reads were aligned with Spliced Transcripts Alignment to a Reference,[37] duplicate reads removed, and gene expression quantified with featureCounts[38] using only uniquely mapping reads. For the Reddy cohort, additional filtering was required to remove abnormally low-coverage samples. Raw count data were normalized with variance stabilizing transformation using DESeq2.[39] For the Schmitz cohort, the gene expression matrix was used in its unmodified form as previously described.[35]

NanoString assay

A subset of tumors in the Arthur cohort were analyzed with the DLBCL90 NanoString assay, as described by Ennishi et al 2019.[40] This CodeSet includes a probe complementary to the exon 7-8 junction in *FCGR2B*, a region that does not share significant sequence similarity with either of its paralogs. RNA was extracted from FFPE biopsies using the Qiagen AllPrep DNA/RNA FFPE kit, and 200 ng was hybridized at 65°C overnight to the DLBCL90 CodeSet probes. Data were normalized for loading and RNA integrity by dividing by the geometric mean of 13 housekeeping genes and multiplying by 1000, followed by $\log_2$ transformation.

FCGR2B qPCR

Oligo(dT)-primed RNA (500 ng) was converted to complementary DNA using the SuperScript III First-Strand Synthesis kit (Life Technologies, Paisley, UK). Quantitative polymerase chain reaction (qPCR) was performed using complementary DNA (24 ng), SuperMix UDG (Life Technologies), and TaqMan probe sets (Life Technologies) targeting *FCGR2B* (Assay ID: Hs01634996_S1) and *HPRT1* (Assay ID: Hs02800695_m1). Thermal cycling was performed using a CFX96 real-time PCR detection system C1000TM (Bio-Rad, Watford, UK). Data were expressed as a ratio of the threshold values for *FCGR2B:HPRT1* and stratified into the following groups based on a cumulative frequency graph: low, cycle quantification value (Cq) $\leq$ .94; medium, Cq .94 to 1.05; and high, Cq $\geq$ 1.05.

Immunohistochemistry staining

FcγRIIB (CD32B) immunohistochemistry (IHC) staining in GOYA was performed using heat-mediated and enzyme antigen retrieval techniques on 4-μm tissue sections cut from paraffin-embedded tissue blocks. Samples were stained with commercially available mAbs using a Bond-Max automated immunostainer with Bond reagents (Leica Microsystems, Milton Keynes, UK). Slides were dewaxed, pretreated with the Bond ER2 protocol, stained with commercially available antibodies, and counterstained with hematoxylin using the standard Bond protocol, according to the manufacturer's instructions. The slides were mounted with Pertex (Histolab products, Germany) and coverslipped with glass coverslips (Surgipath Europe Limited, Cambridge, UK) using a Leica CV5330 (Leica Biosystems, UK). Staining antibodies were diluted in BOND Primary Antibody Diluent (Leica Biosystems) and used at the indicated concentrations: FcγRIIB, clone EP888Y (Abcam, Cambridgeshire, UK), 1/2000 dilution and CD68, clone PG-M1 (DAKO, Agilent Technologies, Cheshire, UK) 1/250 dilution. Images were collected using the Olympus dotSlide microscope system (Olympus, Southend-on-Sea, UK).

IHC staining for the Arthur cohort was as described previously.[34] Tissue microarrays (TMAs) were constructed using duplicate 0.6-mm cores from diagnostic pretreatment FFPE tissue. Staining was performed on the Ventana platform (F. Hoffmann-La Roche, Basel, Switzerland) using routine staining protocols.

IHC expression scoring

In GOYA, tumor expression of FcγRIIB was assessed by light microscopy by 2 individuals, including a pathologist, using a double-headed microscope, with a consensus recorded for each sample. Pathologists and other investigators were blinded to the treatment group when performing the analyses. Scoring thresholds were defined retrospectively while blinded to clinical data. Expression was scored semiquantitatively in comparison with normal mantle cells in reactive tonsil that showed strong membrane staining. Tumors were assessed as negative or positive for membrane staining; the positive staining was graded as strong, moderate, or weak depending on the intensity. The proportion of positive tumor cells was estimated as a percentage of total tumor cells. The staining intensity and percentage of positive tumor cells were amalgamated to give 3 scores, high, low, and negative, defined as follows: membrane staining of at least medium intensity and with $\geq$50% positive cells (high); membrane positive, low intensity or $<$50% positive (low); and cytoplasmic staining or negative membrane staining (negative).

Scoring of FcγRIIB staining of the Arthur cohort TMA was performed as described previously by 2 independent hematopathologists.[34] Intensity and proportion of positive tumor cells were amalgamated into a single score following the same criteria described for GOYA, after taking the average of the scores given by each pathologist.

The numbers of macrophages present within the tumors and their expression of FcγRIIB was assessed in GOYA by double staining TMA sections with CD68 together with FcγRIIB. The total number of $CD68^+$ macrophages and total double-stained macrophages were counted in a standard area for each TMA core. For each core, a single representative field containing predominantly tumor was selected for counting. The macrophages showed granular cytoplasmic staining of CD68 and were only counted if a nucleus was associated with the staining. Double staining was assessed as present if there was identifiable red and brown staining associated with the same nucleus. The percentage of double staining was calculated as the ratio of total double-stained macrophages and total $CD68^+$ macrophages and subsequently split into 3 scores: high (double staining $\geq$50%), low (double-staining $<$50%), and negative (no double-stained macrophages present).

Statistical analysis

The association between *FCGR2B* expression and PFS and overall survival (OS) was assessed separately for each cohort using Kaplan-Meier (KM) plots and Cox regression analysis. For GOYA, the association was evaluated per treatment arm. The predictive analysis in GOYA was performed by assessing treatment effect in patients with low ($\leq$median) and high ($>$median) *FCGR2B* expression and by fitting a model with treatment, *FCGR2B* expression, and an interaction term between treatment and *FCGR2B* expression.

In Cox regression analyses, gene expression was represented as continuous values or dichotomized by the median. KM plots for gene expression were generated using the dichotomized values and

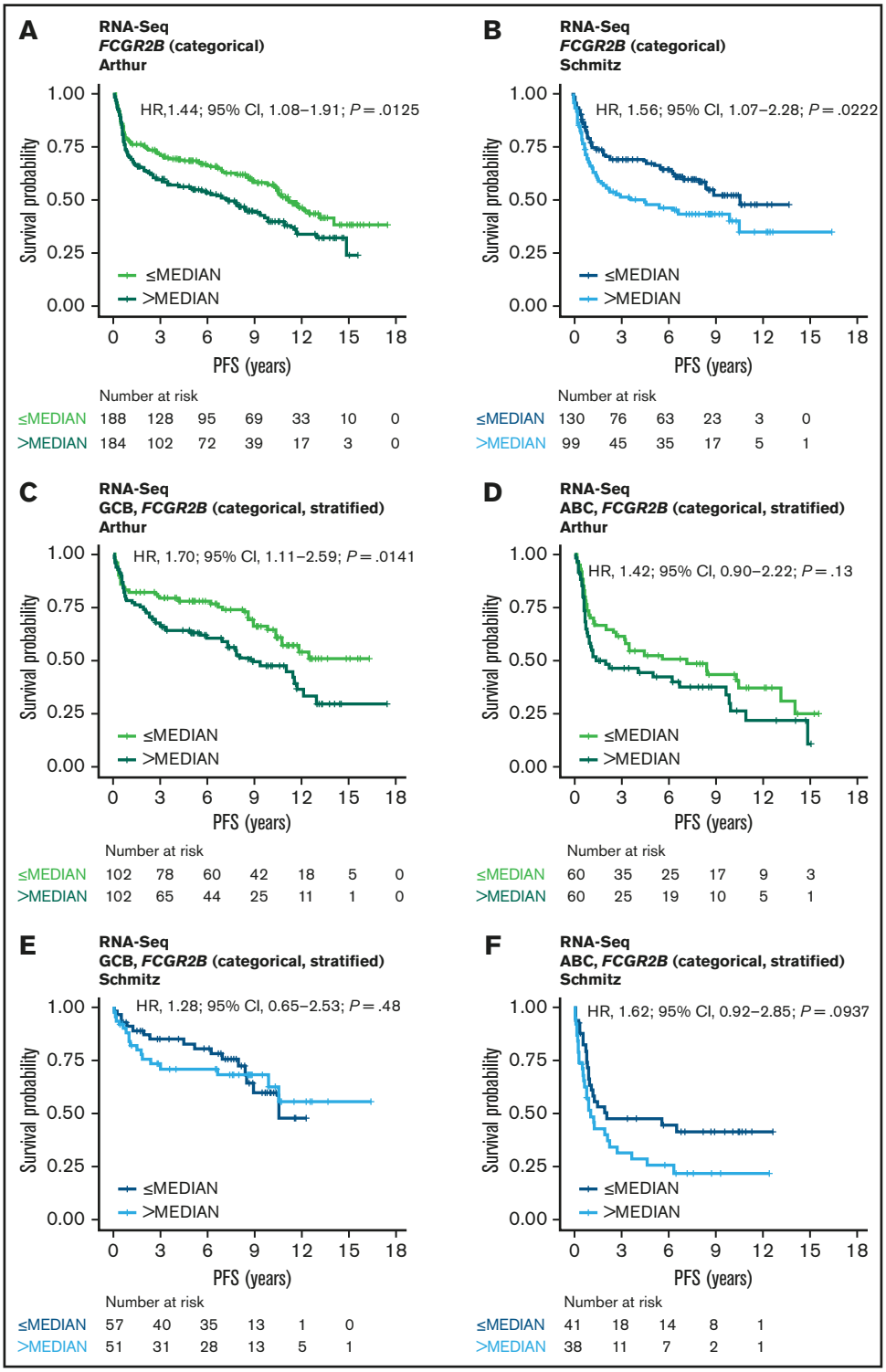

Figure 1. Association of *FCGR2B* expression with PFS in DLBCL patients treated with R-CHOP. Kaplan-Meier curves for PFS in DLBCL based on *FCGR2B* expression measured by (A-B) RNA-seq in the Arthur and Schmitz cohorts and (C-F) according to stratification by COO. Cox regression results based on *FCGR2B* expression dichotomized by median.

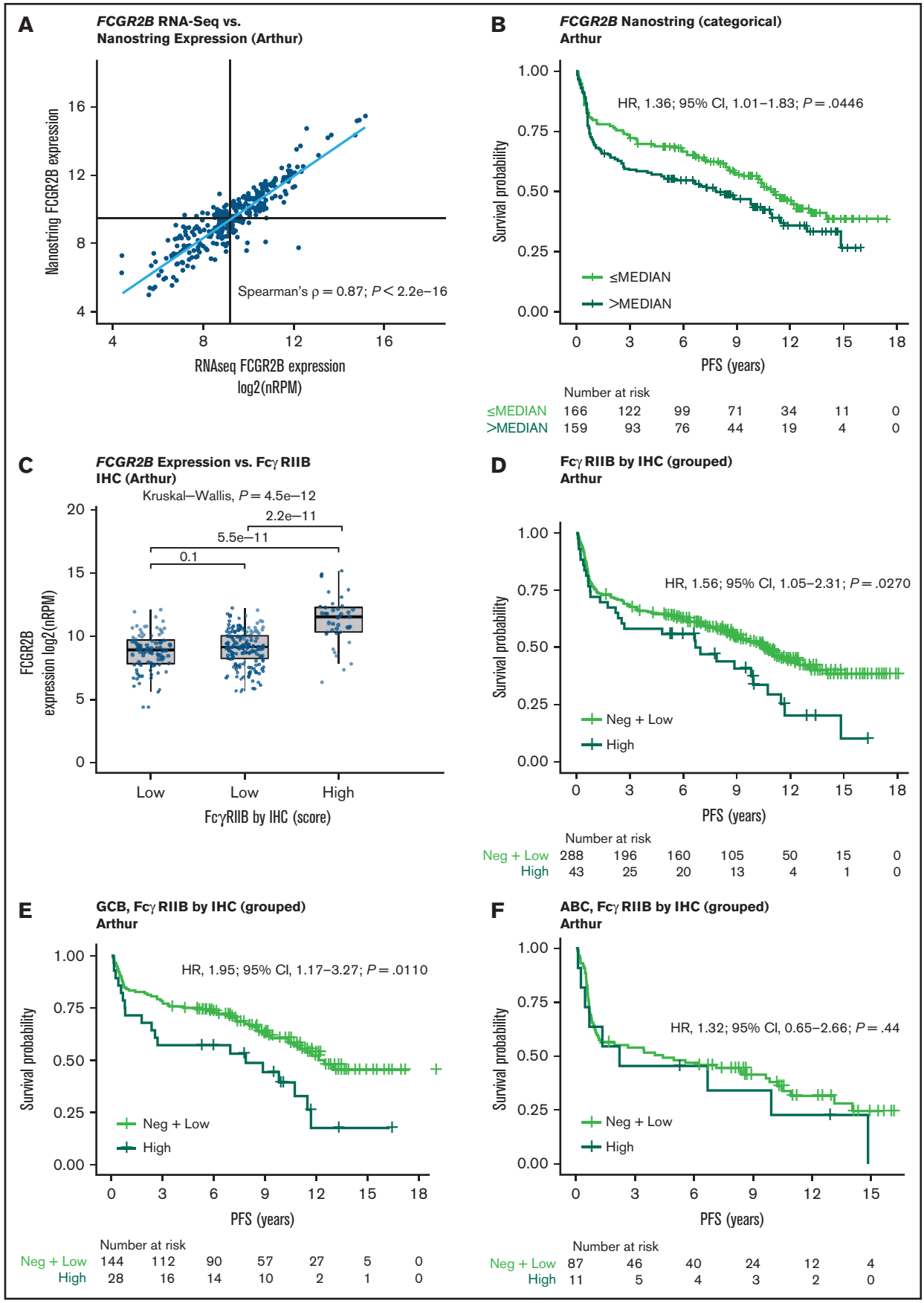
A
FCGR2B RNA-Seq vs. Nanostring Expression (Arthur)
Nanostring FCGR2B expression
RNAseq FCGR2B expression log2(nRPM)
Spearman's ρ = 0.87; P < 2.2e−16
B
FCGR2B Nanostring (categorical) Arthur
HR, 1.36; 95% CI, 1.01–1.83; P = .0446
Survival probability
≤MEDIAN
>MEDIAN
PFS (years)
Number at risk
≤MEDIAN 166 122 99 71 34 11 0
>MEDIAN 159 93 76 44 19 4 0
C
FCGR2B Expression vs. FcγRIIB IHC (Arthur)
Kruskal–Wallis, P = 4.5e−12
2.2e−11
5.5e−11
0.1
FCGR2B expression log2(nRPM)
Low
Low
High
FcγRIIB by IHC (score)
D
FcγRIIB by IHC (grouped) Arthur
HR, 1.56; 95% CI, 1.05–2.31; P = .0270
Survival probability
Neg + Low
High
PFS (years)
Number at risk
Neg + Low 288 196 160 105 50 15 0
High 43 25 20 13 4 1 0
E
GCB, FcγRIIB by IHC (grouped) Arthur
HR, 1.95; 95% CI, 1.17–3.27; P = .0110
Survival probability
Neg + Low
High
PFS (years)
Number at risk
Neg + Low 144 112 90 57 27 5 0
High 28 16 14 10 2 1 0
F
ABC, FcγRIIB by IHC (grouped) Arthur
HR, 1.32; 95% CI, 0.65–2.66; P = .44
Survival probability
Neg + Low
High
PFS (years)
Number at risk
Neg + Low 87 46 40 24 12 4
High 11 5 4 3 2 0

Figure 2.

the corresponding Cox regression statistics (hazard ratio [HR] and *P* values) are displayed.

The prognostic and predictive effect of *FCGR2B* was assessed using univariate and multivariate models. The multivariate model was adjusted for International Prognostic Index (IPI), cell-of-origin (COO), and BCL2 protein expression, which have previously demonstrated prognostic significance in DLBCL.[23,41] *P* values $< .05$ were considered significant.

High-throughput studies

The GOYA RNA sequencing (RNA-seq) data are available at the Gene Expression Omnibus (accession number: GSE125966; https://www.ncbi.nlm.nih.gov/geo/query/acc.cgi?acc=GSE125966).

Results

Association of PFS and OS with expression of *FCGR2B* in patients treated with R-CHOP

RNA-Seq PFS data were available for 372 cases from the Arthur cohort and 229 cases from the Schmitz cohort; RNA-Seq OS data were available for 372 and 234 cases, respectively. RNA-Seq data were available for 454 cases from the Reddy cohort, along with OS but not PFS data. Results from similar analyses using OS are included for all cohorts in the data supplement. Increased *FCGR2B* expression was associated with significantly shorter PFS in the univariate model in both the Arthur and Schmitz cohorts using expression as a dichotomized (Figure 1A-B) and continuous variable (Arthur: HR, 1.09; 95% confidence interval [CI], 1.01-1.19; $P = .0360$; Schmitz: HR, 1.13; 95% CI, 1.02-1.26; $P = .0243$), and was independent of IPI, COO, and BCL2 protein expression in the multivariate model (supplemental Table 2). The KM curves separating according to quartiles of *FCGR2B* expression, and robust effect observed when dichotomizing across a range of thresholds, with respect to the prognostic association with *FCGR2B* expression across the Arthur and Schmitz cohorts, support that this result is independent of the RNA-Seq analysis and quantification methods used (supplemental Figure 1).

Following stratification by COO, the effect of *FCGR2B* expression on PFS was more apparent for the GCB subtype than the activated B-cell (ABC) subtype in the Arthur cohort (univariate analysis [continuous]: GCB: HR, 1.14; 95% CI, 1.03-1.26; $P = .0150$; ABC: HR, 1.09; 95% CI, 0.91-1.31; $P = .36$) (supplemental Table 2; Figure 1C-D). However, in the Schmitz cohort the effect of *FCGR2B* expression was no longer apparent for either the GCB or ABC subtypes (univariate analysis [continuous]: GCB: HR, 1.04; 95% CI, 0.87-1.23; $P = .68$; ABC: HR, 1.14; 95% CI, 0.91-1.43; $P = .25$) (supplemental Table 2; Figure 1E-F).

High *FCGR2B* expression was significantly associated with inferior OS in the Reddy cohort in the continuous univariate model (HR, 1.21; 95% CI, 1.04-1.42; $P = .0167$), although the effect became nonsignificant when adjusting for IPI, COO, and BCL2 by IHC. Weaker OS trends were observed with the Arthur and Schmitz cohorts (supplemental Figure 2; supplemental Table 3).

Validation of the prognostic effect of *FCGR2B* expression by NanoString

NanoString expression data for *FCGR2B* was generated for 325 tumors from the Arthur cohort. Increased *FCGR2B* expression measured by NanoString correlated strongly with *FCGR2B* expression by RNA-seq (Spearman's $\rho = .87$, $P < .0001$) (Figure 2A). The associations of PFS and OS with *FCGR2B* expression by NanoString confirmed those observed by RNA-seq, with high *FCGR2B* expression significantly associated with shorter PFS (univariate analysis [continuous]: HR, 1.13, 95% CI, 1.04-1.23; $P = .0048$) (supplemental Table 4; Figure 2B) but not OS (supplemental Table 4; supplemental Figure 3). These findings were comparable for univariate and multivariate analyses (supplemental Table 4).

Prognostic effect of FcγRIIB protein expression on DLBCL tumors

IHC data on FcγRIIB protein expression were available for 331 patients in the Arthur cohort. Of these, 100 (30%), 188 (58%), and 43 (12%) tumors were FcγRIIB negative, low, and high, respectively. FcγRIIB expression on tumors, measured by IHC, correlated with *FCGR2B* expression observed by RNA-seq with FcγRIIB negative and low samples showing similar *FCGR2B* expression and FcγRIIB high showing significantly higher *FCGR2B* expression (Figure 2C). KM curves of the association of FcγRIIB staining with PFS showed distinct responses corresponding to low and negative FcγRIIB samples (supplemental Figure 4A). The difference in PFS for the high vs the combined negative and low FcγRIIB samples was statistically significant in the overall analysis, with high FcγRIIB samples associated with shorter PFS compared with negative and low FcγRIIB samples (HR, 1.56; 95% CI 1.05-2.31; $P = .0270$; Figure 2D), and when stratified according to COO, remained significant within the GCB (HR, 1.95; 95% CI 1.17-3.27; $P = .0110$) but not ABC DLBCL (Figure 2E-F; supplemental Table 5). Similar trends were observed between OS and FcγRIIB expression but these were not significant (supplemental Figure 4; supplemental Table 6).

Effects of *FCGR2B* expression on prognosis with R-CHOP vs G-CHOP

RNA-seq data were available for 552 patients in the GOYA study. The biomarker-evaluable population (BEP) was comparable with the intent-to-treat population (Table 1) and balanced across treatment arms (supplemental Table 7). Demographic and baseline characteristics for the BEP were similar in the discovery cohorts and GOYA with the exception of the percentage of patients expressing the double-hit signature, which was lower in GOYA than the other cohorts (4.8% vs 19.6%-29.4%). This is consistent with the observation that patients with a greater number of risk factors, including double-

Figure 2. Validation of the *FCGR2B* prognostic effect by NanoString and prognostic effect of FcγRIIB protein expression measured by IHC in the Arthur cohort. (A) Correlation between *FCGR2B* expression measured by NanoString and RNA-Seq. (B) Kaplan-Meier curve for PFS based on *FCGR2B* expression measured by NanoString. Cox regression results based on *FCGR2B* expression dichotomized by median. (C) Correlation of *FCGR2B* expression by RNA-Seq with FcγRIIB protein expression. (D) Kaplan-Meier curves for PFS according to high, low and negative FcγRIIB tumor expression. (E-F) according to stratification by COO. Tumor membrane staining for FcgRIIB was defined as high (at least medium intensity staining with ≥50% positive cells); low (membrane positive, low intensity staining or <50% positive cells) or negative (cytoplasmic staining or negative membrane staining).

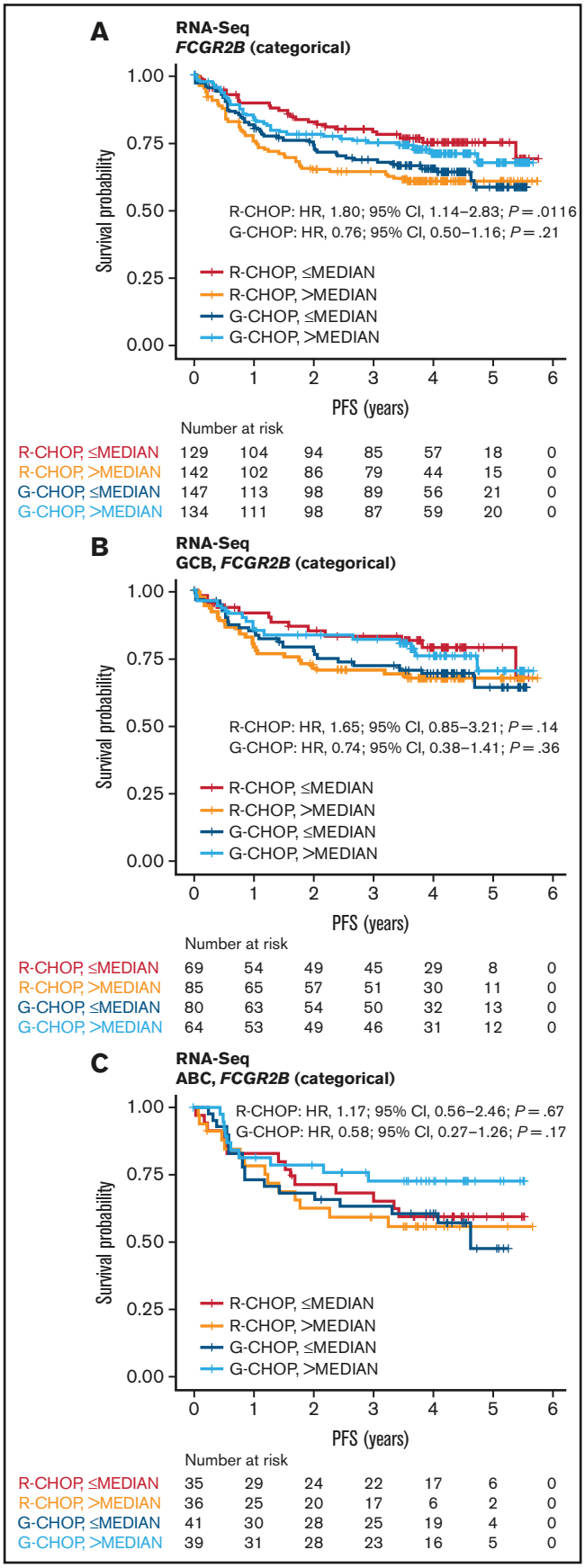

hit lymphomas (ie, with *MYC* and *BCL2* rearrangements) were underrepresented in GOYA (Table 1).

For confirmation, we assayed *FCGR2B* gene expression in 81 of these samples using qPCR and showed good correlation with the RNA-seq measurements ($P = .0465$) (supplemental Figure 5). Importantly, this correlation did not hold with the paralogous *FCGR2C*, as measured by qPCR ($P = .92$), demonstrating that RNA-seq is accurately capturing the expression of *FCGR2B* with little/no contamination from paralogs such as *FCGR2C*.

High *FCGR2B* expression was associated with shorter PFS in R-CHOP-treated (continuous HR, 1.26; 95% CI, 1.00-1.58; $P = .0455$) but not G-CHOP-treated patients (continuous HR, 0.91; 95% CI, 0.69-1.20; $P = .50$) in the univariate analysis (supplemental Table 8; Figure 3A). The effect in R-CHOP-treated patients was supported across various cutoffs and by clear separation between the lowest and highest quartile curves (supplemental Figure 6). A consistent trend was observed after adjustment for IPI, COO, and BCL2 IHC status, but this did not achieve significance (multivariate analysis [continuous]: HR, 1.32; 95% CI, 0.98-1.79; $P = .0695$; supplemental Table 8). Of note, the multivariate analysis had a smaller sample size because of incomplete data for BCL2, which could lead to more variance in the estimated effect size. The effect of *FCGR2B* in R-CHOP-treated patients was similar within the GCB and ABC cohorts and was not significantly different for G-CHOP-treated patients in this stratified analysis (supplemental Table 8; Figure 3B-C).

Patients with higher *FCGR2B* expression appeared to benefit more from G-CHOP than R-CHOP (HR, 0.67; 95% CI, 0.44-1.02; $P = .0622$) vs patients with lower *FCGR2B* expression (HR, 1.58; 95% CI, 1.00-2.50; $P = .0503$), but this did not achieve statistical significance. This trend was supported by the significant treatment:biomarker interaction term ($P = .0064$) in the univariate analysis. A similar effect was observed in the multivariate analysis (interaction term $P = .0249$) (supplemental Table 9). There was also no significant association between *FCGR2B* expression and OS for R-CHOP- or G-CHOP-treated patients in GOYA (supplemental Figure 7; supplemental Table 10).

Prognostic effect of FcγRIIB protein expression in R-CHOP and G-CHOP

FcγRIIB expression data on tumor and macrophages were available for 261 and 249 patients, respectively, in GOYA. Examples of FcγRIIB staining are presented in Figure 4A-B. There was a strong correlation between *FCGR2B* expression by RNA-seq and FcγRIIB expression on tumor cells (Figure 4C). Because of the low frequency of samples expressing low and high tumor FcγRIIB (n = 16 [6.1%] and n = 34 [13.0%], respectively), these samples were merged as FcγRIIB^{+} (as opposed to FcγRIIB^{-}, n = 211 [80.8%]) to enhance power for the subsequent survival analysis. Similarly, for FcγRIIB expression on macrophages, negative (n = 9 [3.6%]) and low (n = 24 [9.6%]) samples were merged into one group for

Figure 3. Association of *FCGR2B* expression by RNA-Seq with PFS for DLBCL patients treated with R-CHOP or G-CHOP in GOYA. Kaplan-Meier curves for PFS based on *FCGR2B* expression measured by (A) RNA-seq in the GOYA cohort and (B-C) according to stratification by COO. Cox regression results based on *FCGR2B* expression dichotomized by median.

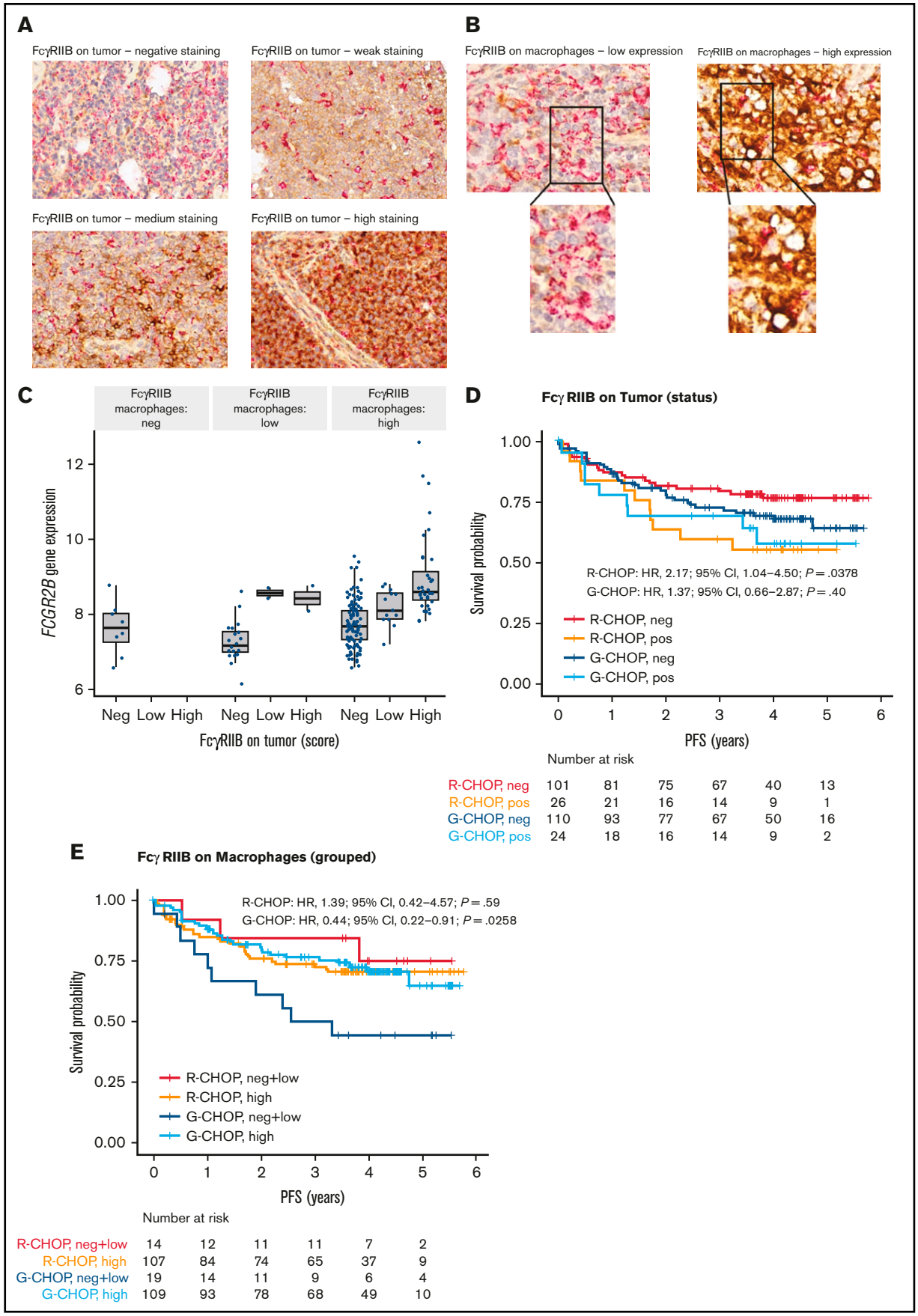
A
FcγRIIB on tumor – negative staining
FcγRIIB on tumor – weak staining
FcγRIIB on tumor – medium staining
FcγRIIB on tumor – high staining
B
FcγRIIB on macrophages – low expression
FcγRIIB on macrophages – high expression
C
FcγRIIB macrophages: neg
FcγRIIB macrophages: low
FcγRIIB macrophages: high
FCGR2B gene expression
12
10
8
6
Neg Low High Neg Low High Neg Low High
FcγRIIB on tumor (score)
D
Fcγ RIIB on Tumor (status)
Survival probability
1.00
0.75
0.50
0.25
0.00
R-CHOP: HR, 2.17; 95% CI, 1.04–4.50; P = .0378
G-CHOP: HR, 1.37; 95% CI, 0.66–2.87; P = .40
R-CHOP, neg
R-CHOP, pos
G-CHOP, neg
G-CHOP, pos
0 1 2 3 4 5 6
PFS (years)
Number at risk
R-CHOP, neg 101 81 75 67 40 13
R-CHOP, pos 26 21 16 14 9 1
G-CHOP, neg 110 93 77 67 50 16
G-CHOP, pos 24 18 16 14 9 2
E
Fcγ RIIB on Macrophages (grouped)
Survival probability
1.00
0.75
0.50
0.25
0.00
R-CHOP: HR, 1.39; 95% CI, 0.42–4.57; P = .59
G-CHOP: HR, 0.44; 95% CI, 0.22–0.91; P = .0258
R-CHOP, neg+low
R-CHOP, high
G-CHOP, neg+low
G-CHOP, high
0 1 2 3 4 5 6
PFS (years)
Number at risk
R-CHOP, neg+low 14 12 11 11 7 2
R-CHOP, high 107 84 74 65 37 9
G-CHOP, neg+low 19 14 11 9 6 4
G-CHOP, high 109 93 78 68 49 10

Figure 4.

comparison with FcγRIIB-high samples (n = 216 [86.8%]). FcγRIIB protein expression on tumor cells correlated with shorter PFS, with a much stronger effect for R-CHOP-treated (HR, 2.17; 95% CI, 1.04-4.50; $P = .0378$) than G-CHOP-treated patients (HR, 1.37; 95% CI, 0.66-2.87; $P = .40$) (Figure 4D; supplemental Table 11). FcγRIIB expression on macrophages did not have a significant effect on PFS in R-CHOP-treated patients; however, among G-CHOP-treated patients, those with high FcγRIIB expression had longer PFS than those with negative/low expression (HR, 0.44; 95% CI, 0.22-0.91; $P = .0258$) (Figure 4E; supplemental Table 11).

There was no significant differential treatment effect for tumors categorized as either FcγRIIB positive or negative (supplemental Table 12), most likely because of low sample size of the FcγRIIB-positive tumor population (n = 50). Analysis of FcγRIIB protein expression stratified by COO was not evaluated because of the small sample size. There was no significant association between FcγRIIB expression on tumors or macrophages and OS (supplemental Figure 8; supplemental Table 13).

Discussion

In the current retrospective analysis, we sought to clarify whether *FCGR2B* messenger RNA and FcγRIIB protein expression were associated with inferior clinical response in large cohorts of patients with DLBCL treated with anti-CD20 mAb-based chemoimmunotherapy. In addition, we determined whether the effects of FcγRIIB were dependent on the anti-CD20 mAb used (R or G).

Using RNA-seq, we determined that *FCGR2B* expression was prognostic for R-CHOP, with high expression associated with shorter PFS in four different cohorts by univariate analysis. This result was robust and independent of the established prognostic biomarkers, IPI, COO, and BCL2 by IHC. In the Arthur cohort, but not the Schmitz or GOYA cohorts, the effect on PFS was more specific to the GCB than to the ABC subtype. This may be explained by the influence of several GCB tumors with high-level amplifications of *FCGR2B* in the Arthur cohort.[34] In part, because of these amplifications, there is a larger dynamic range of *FCGR2B* expression among GCB tumors in the Arthur cohort; the exclusivity of *FCGR2B* amplifications to GCB is likely driven by the different biology of the COO subgroups. Without whole-genome sequencing, we are unable to accurately determine the extent of *FCGR2B* amplifications in the Schmitz cohort. Moreover, high *FCGR2B* expression is only partially explained by genetic alterations, even among cases previously analyzed by whole-genome sequencing.

In the GOYA trial, *FCGR2B* expression was prognostic for R-CHOP but not G-CHOP, providing evidence of a differential effect of FcγRIIB on the impact of different anti-CD20 mAbs. Although no significant association between OS and *FCGR2B* expression was observed in any cohort, OS differences are less commonly observed in such analyses. This lack of association could be attributed to the effect of variable salvage therapies and treatment, and disease-independent deaths, which add noise to OS data. In validating our RNA-seq data, we used qPCR (GOYA) and NanoString (Arthur) to measure *FCGR2B* expression; both methods demonstrated a clear correlation. It is noteworthy that patients with double-hit lymphomas were underrepresented in GOYA because of difficulties in recruiting because these high-risk patients typically require urgent treatment not amenable to the delay between screening and treatment initiation required for trial enrolment.

To understand the basis for this effect, we assessed FcγRIIB protein expression in TMAs from the 2 evaluable cohorts where samples were available (Arthur, n = 297; GOYA, n = 261). In both cohorts, TMA FcγRIIB expression mirrored *FCGR2B* expression by RNA-seq, specifically with regard to expression on the tumor, rather than on tumor-associated macrophages. As such, the prognostic effect observed correlated with FcγRIIB expression levels on the tumor but not on macrophages. These important clinical associations provide further evidence that R is downregulated from the tumor cell surface in the presence of *cis*-mediated FcγRIIB engagement, leading to the loss of R-mediated effector functions. These observations are supported by reports that the lack of FcγRIIb-mediated internalization of G provides for increased phagocytosis of CLL cells.[32] Although previously indicated in small clinical trials of R-chemoimmunotherapy in mantle cell lymphoma,[31] and R monotherapy and maintenance therapy in FL,[42] and supported by extensive preclinical studies,[8,31,33,43] this is the first definitive large clinical trial to show that R, but not G, is negatively affected by FcγRIIB expression on DLBCL tumors. In addition to the small sample size of previous studies, the observation that high FcγRIIB staining is relatively rare (13.0% in both the Arthur cohort and GOYA), may explain why this effect has evaded detection previously. Accordingly, because of validation in several independent cohorts, we propose that FcγRIIB expression could represent a primary predictive biomarker in first-line DLBCL with likely meaningful clinical value. Moreover, although no significant difference was observed between arms when directly compared, our study suggests that simple clinical IHC, qPCR, and/or NanoString analysis could be used, in the absence of RNA-seq, to measure FcγRIIB expression, and help define those patients who are most likely to have impaired clinical response to R and potentially gain more benefit from G. Furthermore, the incorporation of IHC staining of the FcγRIIB protein to establish the tumor specificity of *FCGR2B* expression in this analysis precludes the possibility that *FCGR2B*/FcγRIIB expression is simply a surrogate for the number of immune cells infiltrating the tumor.

In summary, our retrospective analysis demonstrated a clear relationship between *FCGR2B* expression and PFS among patients treated with R-CHOP, providing evidence for this as a potential predictive biomarker in the context of R treatment. No prognostic effect for patients treated with G-CHOP was observed. Higher *FCGR2B* expression was associated with high protein expression on the

Figure 4. Representative IHC staining of tumor TMA and association of FcγRIIB protein expression with PFS for DLBCL patients treated with R-CHOP or G-CHOP in GOYA. TMA sections were stained by IHC for FcγRIIB (brown) and CD68 (red) and assessed by light microscopy. (A) Representative images show ×40 magnification of varying levels of tumor FcγRIIB illustrating negative, weak, medium, and high staining (representative IHC for the Arthur cohort is presented in Arthur et al[34]). (B) Examples of FcγRIIB on macrophages and corresponding ×63 magnification showing low and high expression. (C) Correlation of *FCGR2B* expression by RNA-seq with FcγRIIB protein expression on tumor and macrophages. Kaplan-Meier curves for PFS based on FcγRIIB protein expression on (D) tumors* and (E) macrophages.* *Because of the low number of samples expressing high tumor FcγRIIB, samples expressing high and low FcγRIIB were merged as FcγRIIB$^+$ (as opposed to FcγRIIB$^-$) to gain greater power for the survival analysis. Similarly, for FcγRIIB expression on macrophages, negative and low samples were merged into 1 group.

tumor cells, supporting the previously observed effect of tumor FcγRIIB on R.[8,31] In the future, new therapies such as FcγRIIB-blocking antibodies[41] may be used to target FcγRIIB, and *FCGR2B* expression may be used to facilitate early stratification of patients who would most benefit from treatment with G; however, validation in prospectively designed studies is required to confirm this finding and would be necessary before application to the clinical setting.

Acknowledgments

The authors gratefully acknowledge all patients and clinicians who contributed to this study. This study was sponsored by F. Hoffmann-La Roche Ltd. The authors also thank the Experimental Cancer Medicine Centre (ECMC)–funded University of Southampton, Faculty of Medicine Human Tissue Bank (Human Tissue Authority licence 12009) for sample storage and Federico Mattiello for assisting with the preprocessing of the clinical data in GOYA. The Genomic Variation in Diffuse Large B Cell Lymphomas study was supported by the Intramural Research Program of the National Cancer Institute, National Institutes of Health, Department of Health and Human Services. The datasets have been accessed through the NIH database for Genotypes and Phenotypes (dbGaP). A full list of acknowledgments can be found in the supplementary note (Schmitz et al[35]). Editorial support under the direction of M.N. was provided by Zoe Toland and Louise Profit of Ashfield MedComms, an Ashfield Health company, and funded by F. Hoffmann-La Roche Ltd.

J.C.S. received funding from Bloodwise (11052, 12036), the Kay Kendall Leukaemia Fund (873), and Cancer Research UK (C34999/A18087, ECMC C24563/A15581). M.S.C. and S.A.B. received funding from Cancer Research UK (C11437/A24721). R.D.M. holds an ASH Foundation Junior Scholar award and is a Michael Smith Foundation for Health Research Scholar.

Authorship

Contribution: L.K.H., M.N., R.D.M., and M.S.C. wrote the first draft of the manuscript; M.N., L.K.H., S.A.B., C.K., M.R.-Z., L.H.S., U.V., J.C.S., M.Z.O., R.D.M., and M.S.C. contributed to the study design; M.N., L.K.H., M.A.-K., C.E.H., C.L., R.F., M.J.C., K.N.P., M.R.-Z., M.M., and R.D.M. contributed to the study conduct; C.B., W.K., L.H.S., and M.M. contributed to the recruitment and follow-up of patients; L.K.H., M.A.-K., C.E.H., C.L., R.F., M.J.C., C.B., L.H.S., M.T., and R.D.M. contributed to the data collection; M.N., L.K.H., S.A.B., D.W.S., L.H.S., U.V., C.K.R., G.W.S., P.F., J.C.S., M.Z.O., R.D.M., and M.S.C. contributed to the data analysis; and M.N., L.K.H., C.R.B., A.K., F.M., D.W.S., L.H.S., U.V., M.M., J.C.S., M.Z.O., R.D.M., and M.S.C. interpreted the data.

Conflict-of-interest disclosure: M.N. is an employee of F. Hoffmann-La Roche Ltd. C.L. reports grants from Cancer Research UK and the National Institute of Health Research UK (NIHR). R.F. and M.J.C. report grants from Cancer Research UK and Bloodwise. S.A.B. reports consulting fees from Abbvie, AstraZeneca and Celgene; research funding from Janssen, NanoString and F. Hoffmann-La Roche Ltd; and patents from NanoString. C.R.B. is an employee at Genentech, Inc. and has equity ownership in F. Hoffmann-La Roche Ltd. C.K. is an employee of and has patents and stock ownership of F. Hoffmann-La Roche Ltd. A.K. is an employee of F. Hoffmann-La Roche Ltd. F.M. and M.Z.O. were employees of F. Hoffmann-La Roche Ltd. W.K. reports grants from F. Hoffmann-La Roche Ltd, Amgen, Takeda and Regeneron. D.W.S. reports personal fees from Abbvie and AstraZeneca. L.H.S reports consulting fees from F. Hoffmann-La Roche Ltd, Genentech, Inc, AbbVie, Amgen, Apobiologix, AstraZeneca, Acerta, Celgene, Gilead, Janssen, Kite, Karyopharm, Lundbeck, Merck, Morphosys, Seattle Genetics, Teva, Takeda, T.G. Therapeutics and Verastem; and research funding from F. Hoffmann-La Roche Ltd and Genentech, Inc. U.V. reports personal fees from Celgene, F. Hoffmann-La Roche Ltd, Abbvie, Gilead, Janssen and Regeneron. M.M. reports personal fees from Gilead, Novartis, Janssen and Sandoz; and personal fees and travel fees from F. Hoffmann-La Roche Ltd and Servier. M.T. reports personal fees from Janssen, Gilead Sciences, Takeda, B.M.S., Amgen, Abbvie, F. Hoffmann-La Roche Ltd, Null, MorphSys, Incyte and Celgene. C.K.R. reports grant fees from Terry Fox Research Institute. G.W.S. reports fees from Seattle Genetics Inc. J.C.S. reports research funding from F. Hoffmann-La Roche Ltd and Cambridge Epigenetix. R.D.M. reports personal fees from Celgene. M.S.C. reports grants from Cancer Research UK and Bloodwise; and grants, personal fees and patents from Bioinvent. The remaining authors declare no competing financial interests.

The current affiliation for C.E.H. is Nuffield Department of Medicine, John Radcliffe Hospital, University of Oxford, Oxford, United Kingdom.

The current affiliation for M.Z.O. is Novo Nordisk, Zurich, Switzerland.

ORCID profiles: L.K.H., 0000-0002-6413-6586; M.A.-K., 0000-0002-7451-363X; C.L., 0000-0002-4701-5213; M.R.-Z., 0000-0002-1064-5350; W.K., 0000-0001-7208-4117; U.V., 0000-0001-7772-2747; M.T., 0000-0002-6952-6073; C.R., 0000-0001-6306-9361; P.F., 0000-0001-9364-9391; J.C.S., 0000-0002-0972-2881; R.D.M., 0000-0003-2932-7800; M.S.C., 0000-0003-2077-089X

Correspondence: Mark S. Cragg, Antibody and Vaccine Group, Centre for Cancer Immunology, School of Cancer Sciences, University of Southampton, Faculty of Medicine, Southampton General Hospital, Tremona Rd, Southampton, SO16 6YD, United Kingdom; e-mail: m.s.cragg@soton.ac.uk.

References

1. Edwards JC, Cambridge G. B-cell targeting in rheumatoid arthritis and other autoimmune diseases. *Nat Rev Immunol*. 2006;6(5):394-403.

2. Lim SH, Beers SA, French RR, Johnson PW, Glennie MJ, Cragg MS. Anti-CD20 monoclonal antibodies: historical and future perspectives. *Haematologica*. 2010;95(1):135-143.

3. Marshall MJE, Stopforth RJ, Cragg MS. Therapeutic antibodies: what have we learnt from targeting CD20 and where are we going? *Front Immunol*. 2017;8:1245.

4. Sopp J, Cragg MS. Deleting malignant B cells with second-generation anti-CD20 antibodies. *J Clin Oncol*. 2018;36(22):2323-2325.

5. Uchida J, Hamaguchi Y, Oliver JA, et al. The innate mononuclear phagocyte network depletes B lymphocytes through Fc receptor-dependent mechanisms during anti-CD20 antibody immunotherapy. *J Exp Med*. 2004;199(12):1659-1669.

6. Minard-Colin V, Xiu Y, Poe JC, et al. Lymphoma depletion during CD20 immunotherapy in mice is mediated by macrophage FcgammaRI, FcgammaRIII, and FcgammaRIV. *Blood*. 2008;112(4):1205-1213.

7. Beers SA, French RR, Chan HT, et al. Antigenic modulation limits the efficacy of anti-CD20 antibodies: implications for antibody selection. *Blood*. 2010;115(25):5191-5201.

8. Tipton TR, Roghanian A, Oldham RJ, et al. Antigenic modulation limits the effector cell mechanisms employed by type I anti-CD20 monoclonal antibodies. *Blood*. 2015;125(12):1901-1909.

9. Gül N, Babes L, Siegmund K, et al. Macrophages eliminate circulating tumor cells after monoclonal antibody therapy. *J Clin Invest*. 2014;124(2):812-823.

10. Sica A, Schioppa T, Mantovani A, Allavena P. Tumour-associated macrophages are a distinct M2 polarised population promoting tumour progression: potential targets of anti-cancer therapy. *Eur J Cancer*. 2006;42(6):717-727.

11. Biswas SK, Allavena P, Mantovani A. Tumor-associated macrophages: functional diversity, clinical significance, and open questions. *Semin Immunopathol*. 2013;35(5):585-600.

12. Lehmann B, Biburger M, Brückner C, et al. Tumor location determines tissue-specific recruitment of tumor-associated macrophages and antibody-dependent immunotherapy response. *Sci Immunol*. 2017;2(7):eaah6413.

13. McCord R, Bolen CR, Koeppen H, et al. PD-L1 and tumor-associated macrophages in de novo DLBCL. *Blood Adv*. 2019;3(4):531-540.

14. Nimmerjahn F, Ravetch JV. Fcgamma receptors as regulators of immune responses. *Nat Rev Immunol*. 2008;8(1):34-47.

15. Burgess M, Mapp S, Mazzieri R, et al. Increased FcγRIIB dominance contributes to the emergence of resistance to therapeutic antibodies in chronic lymphocytic leukaemia patients. *Oncogene*. 2017;36(17):2366-2376.

16. Klanova M, Oestergaard MZ, Trněný M, et al. Prognostic impact of natural killer cell count in follicular lymphoma and diffuse large B-cell lymphoma patients treated with immunochemotherapy. *Clin Cancer Res*. 2019;25(15):4634-4643.

17. Pawluczkowycz AW, Beurskens FJ, Beum PV, et al. Binding of submaximal C1q promotes complement-dependent cytotoxicity (CDC) of B cells opsonized with anti-CD20 mAbs ofatumumab (OFA) or rituximab (RTX): considerably higher levels of CDC are induced by OFA than by RTX. *J Immunol*. 2009;183(1):749-758.

18. van Imhoff GW, McMillan A, Matasar MJ, et al. Ofatumumab versus rituximab salvage chemoimmunotherapy in relapsed or refractory diffuse large B-cell lymphoma: the ORCHARRD study. *J Clin Oncol*. 2017;35(5):544-551.

19. Maloney DG, Ogura M, Fukuhara N, et al. A phase 3 randomized study (HOMER) of ofatumumab vs rituximab in iNHL relapsed after rituximab-containing therapy. *Blood Adv*. 2020;4(16):3886-3893.

20. Goede V, Fischer K, Busch R, et al. Obinutuzumab plus chlorambucil in patients with CLL and coexisting conditions. *N Engl J Med*. 2014;370(12):1101-1110.

21. Hiddemann W, Barbui AM, Canales MA, et al. Immunochemotherapy with obinutuzumab or rituximab for previously untreated follicular lymphoma in the GALLIUM study: influence of chemotherapy on efficacy and safety [published correction appears in *J Clin Oncol*. 2018;36(27):2815]. *J Clin Oncol*. 2018;36(23):2395-2404.

22. Marcus R, Davies A, Ando K, et al. Obinutuzumab for the first-line treatment of follicular lymphoma. *N Engl J Med*. 2017;377(14):1331-1344.

23. Vitolo U, Trněný M, Belada D, et al. Obinutuzumab or rituximab plus cyclophosphamide, doxorubicin, vincristine, and prednisone in previously untreated diffuse large B-cell lymphoma. *J Clin Oncol*. 2017;35(31):3529-3537.

24. Sehn LH, Martelli M, Trněný M, et al. Final analysis of GOYA: a randomized, open-label, phase III study of obinutuzumab or rituximab plus CHOP in patients with previously untreated diffuse large B-cell lymphoma. *Blood*. 2019;134(suppl 1):4088.

25. Cragg MS, Morgan SM, Chan HT, et al. Complement-mediated lysis by anti-CD20 mAb correlates with segregation into lipid rafts. *Blood*. 2003;101(3):1045-1052.

26. Teeling JL, French RR, Cragg MS, et al. Characterization of new human CD20 monoclonal antibodies with potent cytolytic activity against non-Hodgkin lymphomas. *Blood*. 2004;104(6):1793-1800.

27. Ivanov A, Beers SA, Walshe CA, et al. Monoclonal antibodies directed to CD20 and HLA-DR can elicit homotypic adhesion followed by lysosome-mediated cell death in human lymphoma and leukemia cells. *J Clin Invest*. 2009;119(8):2143-2159.

28. Alduaij W, Ivanov A, Honeychurch J, et al. Novel type II anti-CD20 monoclonal antibody (GA101) evokes homotypic adhesion and actin-dependent, lysosome-mediated cell death in B-cell malignancies. *Blood*. 2011;117(17):4519-4529.

29. Herter S, Herting F, Mundigl O, et al. Preclinical activity of the type II CD20 antibody GA101 (obinutuzumab) compared with rituximab and ofatumumab in vitro and in xenograft models. *Mol Cancer Ther*. 2013;12(10):2031-2042.

30. Mössner E, Brünker P, Moser S, et al. Increasing the efficacy of CD20 antibody therapy through the engineering of a new type II anti-CD20 antibody with enhanced direct and immune effector cell-mediated B-cell cytotoxicity. *Blood*. 2010;115(22):4393-4402.

31. Lim SH, Vaughan AT, Ashton-Key M, et al. Fc gamma receptor IIb on target B cells promotes rituximab internalization and reduces clinical efficacy. *Blood*. 2011;118(9):2530-2540.

32. Elias S, Kahlon S, Kotzur R, Kaynan N, Mandelboim O. Obinutuzumab activates FcγRI more potently than other anti-CD20 antibodies in chronic lymphocytic leukemia (CLL). *OncoImmunology*. 2018;7(6):e1428158.

33. Vaughan AT, Iriyama C, Beers SA, et al. Inhibitory FcγRIIb (CD32b) becomes activated by therapeutic mAb in both cis and trans and drives internalization according to antibody specificity. *Blood*. 2014;123(5):669-677.

34. Arthur SE, Jiang A, Grande BM, et al. Genome-wide discovery of somatic regulatory variants in diffuse large B-cell lymphoma. *Nat Commun*. 2018;9(1):4001.

35. Schmitz R, Wright GW, Huang DW, et al. Genetics and pathogenesis of diffuse large B-cell lymphoma. *N Engl J Med*. 2018;378(15):1396-1407.

36. Reddy A, Zhang J, Davis NS, et al. Genetic and functional drivers of diffuse large B cell lymphoma. *Cell*. 2017;171(2):481-494.e15.

37. Dobin A, Davis CA, Schlesinger F, et al. STAR: ultrafast universal RNA-seq aligner. *Bioinformatics*. 2013;29(1):15-21.

38. Liao Y, Smyth GK, Shi W. featureCounts: an efficient general purpose program for assigning sequence reads to genomic features. *Bioinformatics*. 2014;30(7):923-930.

39. Love MI, Huber W, Anders S. Moderated estimation of fold change and dispersion for RNA-seq data with DESeq2. *Genome Biol*. 2014;15(12):550.

40. Ennishi D, Jiang A, Boyle M, et al. Double-hit gene expression signature defines a distinct subgroup of germinal center B-cell-like diffuse large B-cell lymphoma. *J Clin Oncol*. 2019;37(3):190-201.

41. Tsuyama N, Sakata S, Baba S, et al. BCL2 expression in DLBCL: reappraisal of immunohistochemistry with new criteria for therapeutic biomarker evaluation. *Blood*. 2017;130(4):489-500.

42. Lee CS, Ashton-Key M, Cogliatti S, et al. Expression of the inhibitory Fc gamma receptor IIB (FCGR2B, CD32B) on follicular lymphoma cells lowers the response rate to rituximab monotherapy (SAKK 35/98). *Br J Haematol*. 2015;168(1):145-148.

43. Roghanian A, Teige I, Mårtensson L, et al. Antagonistic human FcγRIIB (CD32B) antibodies have anti-tumor activity and overcome resistance to antibody therapy in vivo. *Cancer Cell*. 2015;27(4):473-488.